ChemPubSoc Europe

DOI: 10.1002/open.201402135

Open Access ChemistryOPEN Communications

Self-Assembled Functionalized Graphene Nanoribbons from Carbon Nanotubes

Eunice Cunha,[a] Maria Fernanda Proença,[b] Florinda Costa,[c] António J. Fernandes,[c] Marta A. C. Ferro,[d] Paulo E. Lopes,[e] Mariam González-Debs,[f] Manuel Melle-Franco,[g] Francis Leonard Deepak,[f] and Maria C. Paiva*[a]

Graphene nanoribbons (GNR) were generated in ethanol solution by unzipping pyrrolidine-functionalized carbon nanotubes under mild conditions. Evaporation of the solvent resulted in regular few-layer stacks of graphene nanoribbons observed by transmission electron microscopy (TEM) and X-ray diffraction. The experimental interlayer distance (0.49–0.56 nm) was confirmed by computer modelling (0.51 nm). Computer modelling showed that the large interlayer spacing (compared with graphite) is due to the presence of the functional groups and depends on their concentration. Stacked nanoribbons were observed to redissolve upon solvent addition. This preparation method could allow the fine-tuning of the interlayer distances by controlling the number and/or the nature of the chemical groups in between the graphene layers.

The formation of stable graphene suspensions is a topic of great interest that has been the focus of recent investigations. Different approaches proposed in the literature comprise the exfoliation of graphite in high-boiling-point solvents,[1] the formation of graphene oxide (GO) followed by its reduction in solution (RGO),[2,3] or the formation of graphene nanoribbons (GNR) from carbon nanotubes (CNT) using a similar oxidation approach.[4] The formation of GNR from CNT is of particular interest, and different protocols involving reactive chemical species such as oxidants and radicals have been reported for the controlled cutting of CNT, typically requiring ultrasonication, or another energy source, at high power for long periods of time.[4–9]

The oxidative approaches for CNT unzipping described so far have advantages and downsides; an example of the former being the high yield of GNR provided by some of the methods, and of the latter related to the production of highly defective graphene due to the extensive oxidation/reduction processes and high energy requirements. Only a few non-oxidative methods for CNT unzipping, that lead to reasonable yields are reported. Kumar et al.[10] reported the unzipping of multi-wall CNT by excimer laser irradiation, pointing out the contribution of defect sites for the unzipping process. Other approaches include lithium intercalation,[5] and catalytic unzipping using palladium and microwave irradiation.[6]

Inspired by the observation of the unzipping of functionalized CNT under ultra-high vacuum scanning tunneling microscopy (UHV STM),[11] where the type of functionalization plays a key role in the unzipping process,[12] an alternative method to produce GNR in solution was developed. The CNT were functionalized by the 1,3-dipolar cycloaddition reaction of azomethine ylides, and their surface characterization was described elsewhere[13] (in addition, thermogravimetric analysis (TGA) and transmission electron microscopy (TEM) of the CNT are presented as Supporting Information). The unzipping of the functionalized layer was achieved in ethanol solution, producing stable suspensions of GNR. In the present work, we report the stacking of the functionalized GNR obtained from large and small diameter functionalized CNT upon solvent evaporation, generating stacks with a large interlayer spacing required to accommodate the functional groups at the GNR surface, as confirmed by molecular modelling.

The UV-visible absorption spectra obtained for the GNR solutions are presented in Figure 1. The spectra of the solutions of GNR NC7000 and GNR MWNT SA (GNR formed by unzipping of nanotubes NC7000 and MWNT SA, respectively, see Experimental Section) show two shoulders, at approximately 250 nm and 300 nm, similar to the spectra of graphene oxide nanosheets reported elsewhere.[3,14] These signals were considered indica-

[a] E. Cunha, Dr. M. C. Paiva
Institute for Polymers and Composites/I3N, University of Minho, Campus of Azurem, 4800-058 Guimarães (Portugal)
E-mail: mcpaiva@dep.uminho.pt

[b] Prof. M. F. Proença
Department of Chemistry, University of Minho, Campus of Gualtar, 4710-057 Braga (Portugal)

[c] Prof. F. Costa, A. J. Fernandes
Physics of Semiconductors, Optoelectronics & Disordered Systems/I3N, University of Aveiro, 3810-193 Aveiro (Portugal)

[d] M. A. C. Ferro
CICECO, Department of Ceramics & Glass Engineering, University of Aveiro, 3810-193 Aveiro (Portugal)

[e] Dr. P. E. Lopes
PIEP-Pole for Innovation in Polymer Engineering, University of Minho, Campus of Azurém, 4800-058 Guimarães (Portugal)

[f] Dr. M. González-Debs, Dr. F. L. Deepak
International Iberian Nanotechnology Laboratory (INL), Av. Mestre José Veiga, 4715-330 Braga (Portugal)

[g] Dr. M. Melle-Franco
Computer Science & Technology Center, University of Minho, Campus of Gualtar, 4710-057 Braga (Portugal)

Supporting information for this article is available on the WWW under http://dx.doi.org/10.1002/open.201402135.

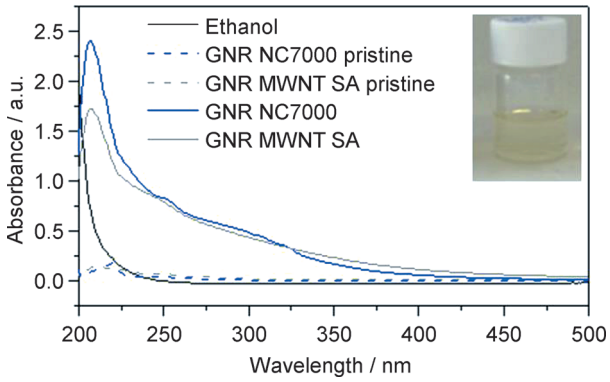

Figure 1. UV-visible spectra of graphene nanoribbon (GNR) solutions produced from pristine and functionalized NC7000 and MWNT SA, in ethanol. The insert shows a picture of the solution of GNR NC7000 in ethanol.

tive of the presence of graphene nanoribbons in solution. The spectra obtained for the blank tests (Figure 1) reveal an absorption spectrum similar to that of the solvent near a λ value of 230 nm indicating that the sonication process does not induce the unzipping of the pristine CNTs, or the formation of a detectable amount GNR. The weight absorptivity of the GNR in solution was measured by UV-visible spectroscopy at 250 nm, and the values determined were $1600 \pm 200\ L\,g^{-1}\,m^{-1}$ for the GNR from f-NC7000 (GNR NC7000) and $2000 \pm 100\ L\,g^{-1}\,m^{-1}$ for the GNR from f-MWNT SA (GNR MWNT SA). These results are in the same range of values reported in the literature for graphene solutions.[1,3] GNR concentrations of 50 and 40 mg L^{-1} were measured for the solutions obtained by ultrasonication of f-NC7000 and f-MWNT SA in ethanol, respectively.

GNR were deposited from solution on silicon wafers, as well as samples of NC7000 and MWNT SA and analyzed by Raman spectroscopy. The acquired Raman data were typical of an sp2 hybridized carbon atom, as illustrated in Figure 2 for all the systems studied. For the carbon nanotubes, the G and D bands appear as prominent features compared with a weaker 2D band. Notably, the spectrum of MWNT SA shows intense G and 2D bands, and a smaller D band indicating that these large diameter nanotubes have lower defect contents.[15] The spectra obtained for GNR shows a sharp intense symmetric G band and an asymmetric and blue-shifted 2D band, typical of the formation of few-layer GNRs. This result is compatible with the stacking of the GNR deposited by solvent evaporation.[16]

TEM images of samples obtained from concentrated ethanol solutions show the presence of films that likely arise from GNR agglomeration during solvent evaporation. The films from GNR NC7000 samples form smaller domains (Figure 3a) compared with those from GNR MWNT SA samples (Figure 3d).

Images from GNR NC7000 were obtained on a 80 kV high-resolution transmission electron microscope (HRTEM) and showed areas with few layers of graphene, such as represented in Figure 3b. Fast Fourier transforms (FFT) obtained at the spot marked with A, shown in Figure 3c, revealed hexagonal patterns typical of graphene. GNR MWNT SA present larger ribbons, and their stacks were robust enough to be imaged on a 200 kV TEM (Figure 3d,e). The TEM image of Figure 3e shows the presence of large stacks of GNR that hamper the observation of the 110 graphene plane. Magnification of the image at the spot marked B illustrates the GNR stacking through the regularly spaced parallel lines (Figure 3f). The FFT pattern obtained at the spot marked B, shown in Figure 3g, provides a measure of the interlayer spacing of approximately 0.49 nm. The micrographs also show remaining CNT fragments entangled in the GNR formed.

X-rays diffraction of GNR NC7000 and GNR MWNT SA was performed on samples deposited on glass slides by solvent evaporation. The X-ray intensity profiles for both GNR NC7000 and GNR MWNT SA exhibited a single peak at 31.68° (2θ). This peak is not present on the starting functionalized CNT material (Figure 4). The peak obtained for GNR MWNT SA is sharper than the peak of the GNR NC7000.

Molecular models were applied to study the effect of the functionalization degree in the interlayer distance (Figure 5). Interestingly, very similar distances were found for the highest functionalization densities, namely 0.54–0.51 nm for 8–72 graphene layer carbon atoms per functional group. In contrast, lowering the concentration abruptly decreases the interlayer distance to 0.41 nm for 98 carbon atoms per functional group. This is due to the fact that, at lower densities, the graphene

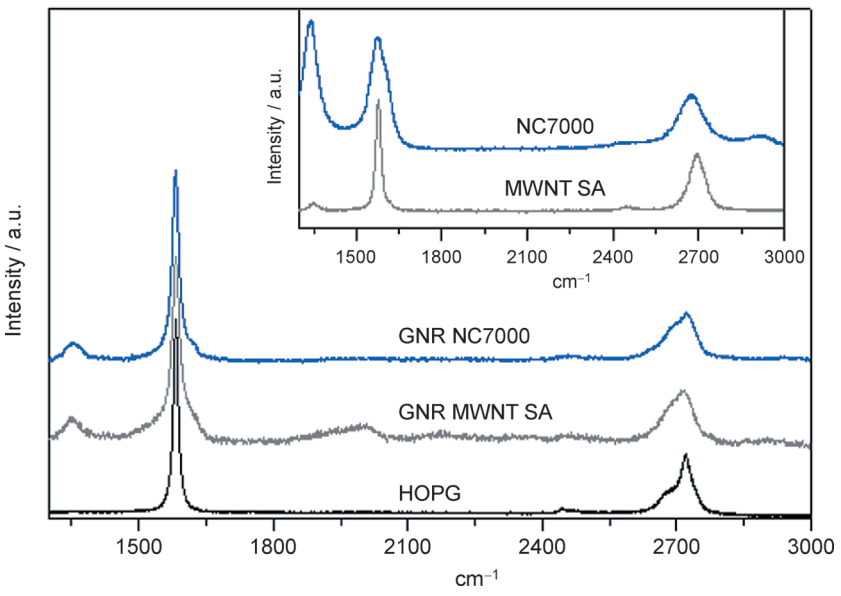

Figure 2. Raman spectra of the carbon nanotubes (CNT) (insert) and of graphene nanoribbons (GNR) deposited on silicon from ethanol solutions. Highly ordered pyrolytic graphite (HOPG) spectrum is included for comparison.

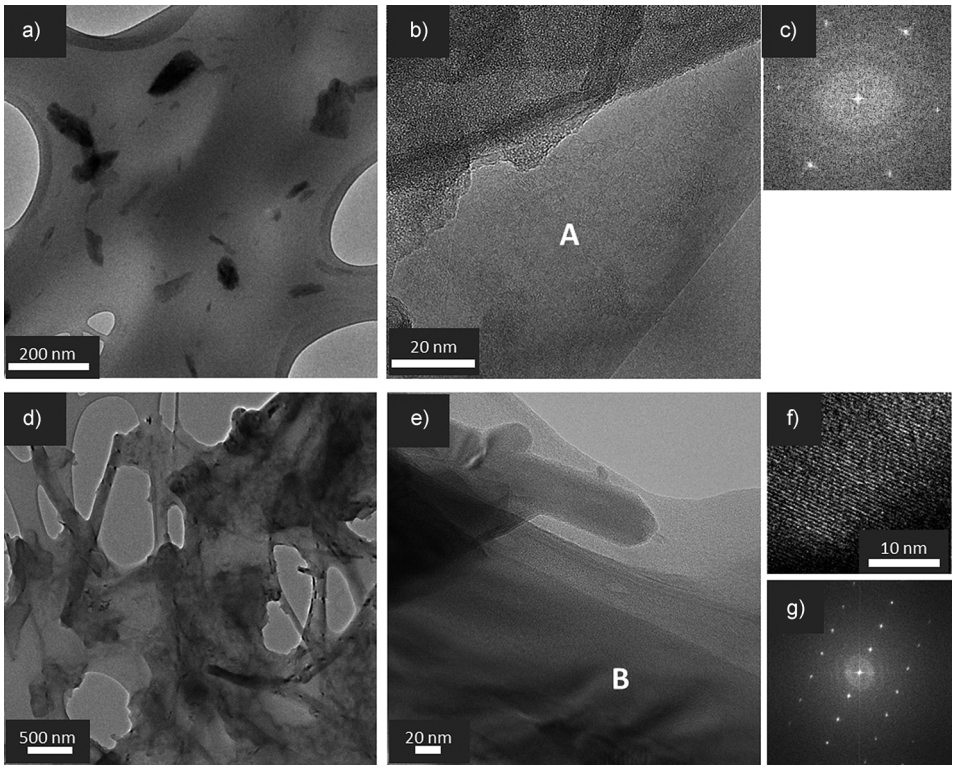

Figure 3. Transmission electron microscopy (TEM) micrographs of graphene nanoribbon (GNR) formed in ethanol by unzipping of NC7000 (a,b) and MWNT SA (d,e); Fast Fourier transforms (FFT) calculated on the area A, for GNR NC7000, and B for GNR MWNT SA are shown in c) and g), respectively; magnification of the area B in micrograph e) showing the regular pattern (f).

sheets are able to flex to accommodate the functional groups, decreasing more efficiently the interlayer density. By further decreasing the functional group concentration, the graphite spacing is asymptotically approached. At the experimental functional group concentration of 1 group per 50 graphene carbon atoms, an interlayer distance of 0.51 nm is obtained (Figure 6).

Considering the structure found with molecular modelling (Figure 6), the X-ray diffraction peak observed can be assigned to the 002 set of crystallographic planes considering the *c* dimension of the unit cell defined as the graphene-to-graphene interlayer distance. From the X-ray data, this distance is calculated to be 0.56 nm, which is close to the estimated values from molecular modeling, 0.51 nm, and to the value of 0.49 nm measured from TEM

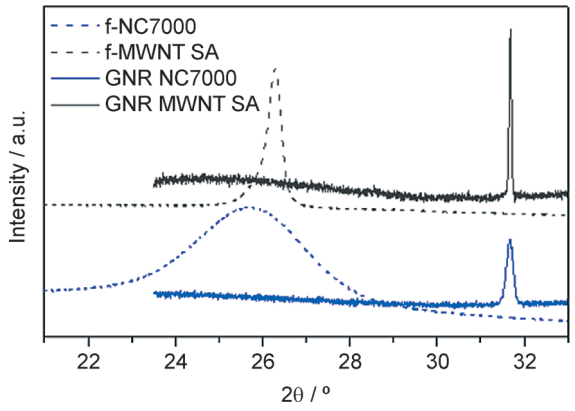

Figure 4. X-ray intensity profiles of graphene nanoribbon (GNR) NC7000 and GNR MWNT SA deposited on glass lamella from ethanol solutions (——), and of the corresponding carbon nanotube (CNT) starting material (-----).

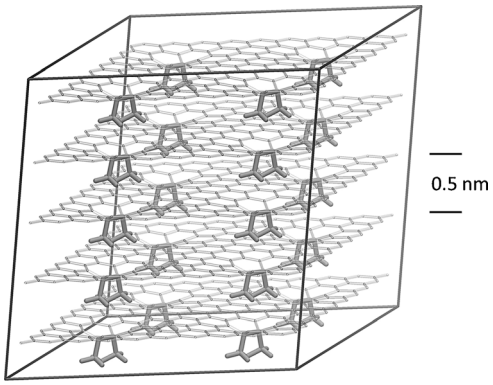

Figure 6. Computer model of functionalized graphene; one functional group per 50 graphene carbon atoms.

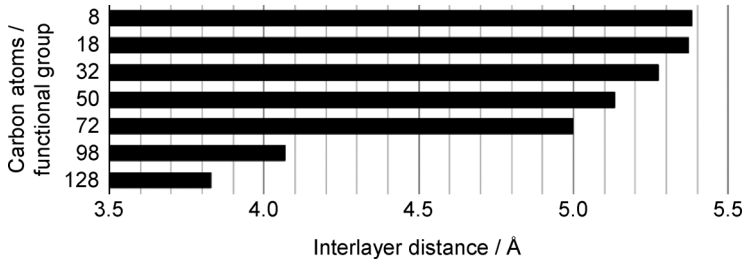

Figure 5. Average interlayer distance (Å) versus functional group concentration (number of graphene carbon atoms per functional group).

micrographs. The average number of graphene layers in these self-assembled stackings, calculated from the X-ray crystallite thickness, is 2–3 for GNR NC7000 and 5–6 for GNR MWNT SA.

It should be remarked that GNR deposited by solvent evaporation remain soluble, that is, addition of ethanol to the deposited GNR leads to their complete re-solubilization. This phenomenon is probably associated with the larger separation between graphene sheets that allow solvent molecules to readily

enter the interlayer void space (see Figure 6) facilitating the exfoliation.

In summary, self-assembled GNR stacks were observed and characterized by TEM, X-ray diffraction and Raman spectroscopy. The GNR were successfully produced in solution by unzipping of functionalized CNT of different diameters. The CNT were functionalized with pyrrolidine-type groups, generating pyrrolidine-functionalized GNR. Raman spectroscopy evidenced the sp2 character of the GNR. TEM illustrated the formation of larger GNR from CNT with larger diameter, and a tendency of the deposited GNR to form regular stacks with an interlayer distance of approximately 0.5 nm. The formation of regular stacks was confirmed by X-ray diffraction, calculating the stack length as 2–3 GNR layers when formed from NC7000, and 5–6 GNR layers when formed from MWNT SA. Computer models estimated interlayer distances of similar magnitude and showed that the interlayer distances depend on the concentration of functional groups. The GNR stacks formed by solvent evaporation were easily redissolved after solvent addition.

Experimental Section

Two types of CNT were investigated, NC7000 from Nanocyl and MWNT SA from Sigma–Aldrich (catalog reference 659258), both produced by chemical vapor deposition (CVD). NC7000 has a diameter of 7–10 nm, and MWNT SA has a diameter of 110–170 nm. The CNT were functionalized by a 1,3-dipolar cycloaddition reaction of azomethine ylides using a one-pot functionalization procedure described elsewhere[13] leading to the formation of pyrrolidine-type groups bonded to the CNT surface. The functionalization was carried out at 250 °C over 5 h.

The unzipping of the CNT was performed using an Ultrasonic processor UP100H from Hielscher, equipped with a sonotrode MS2. CNT suspensions were prepared by mixing functionalized CNT (5 mg) in ethanol (8 mL). A control experiment was conducted using pristine CNT (5 mg) in ethanol (8 mL). Ultrasound energy was applied to the suspensions during 15 min at maximum power. The suspensions were centrifuged (8000 rpm, 1 h) to separate the unzipped CNT, and the GNR supernatant solutions were collected. These solutions were analyzed by UV-visible spectroscopy on a Shimadzu UV-240 1 PC, using 10 mm light path quartz cells.

The micro-Raman analysis was conducted in the backscattering configuration on a Jobin Yvon HR800 instrument (Horiba, Japan), using a 1800 L mm^{-1} grating and the 532 nm laser line from a Nd:YAG DPSS laser (Ventus, Laser Quantum, UK). A 50x objective (spot size: ~3 μm, NA = 0.75, Olympus, Japan) was used to focus the laser light onto the sample (< 0.15 mW μm^{-2}) and to collect the backscattered Raman radiation to be detected by a Peltier cooled (223 K) CCD sensor. The spectrometer was operated in the confocal mode, setting the iris to 300 μm, while the acquisition time was set to 30 s with 2 accumulations.

Transmission electron microscopy (TEM) of the GNR MWNT SA was performed on an Energy Filtered 200 kV Transmission Electron Microscope HR-(EF)TEM–JEOL 2200FS. TEM analysis of the GNR NC7000 was carried out on a Titan ChemiSTEM 80–200 kV probe Cs corrected microscope. Low-magnification TEM and high-resolution TEM (HRTEM) images were acquired with a GATAN Ultrascan 1000 P camera controlled with digital micrograph software integrated in the microscope's user interface. The samples were prepared by adding a drop of the GNR solution onto a lacey carbon Cu grid (300 mesh, Ted Pella) and allowing it to dry under vacuum.

X-rays diffraction experiments were performed on a PANalytical X'Pert PRO XRD system using the Cu Kα1 wavelength of 0.15406 nm from a copper X-ray tube operated at 45 kV and 40 mA. A PIXcel-3D detector was used, and the scan range was from 4 to 40° in 2θ. The GNR samples were deposited on glass lamellae by solvent evaporation.

The unzipping process produces functionalized GNRs with widths equal or larger than 35 nm for GNR NC7000 and 350 nm for GNR MWNT SA. For this reason, a model of functionalized graphene (see Figure 6), as opposite to finite GNR, was chosen. Graphene layers and their intermolecular interactions were modelled with the MM3 force field that has been found to give accurate intermolecular structures.[17] All the calculations were performed with the TINKER molecular mechanics suite[18] using three-dimensional periodic boundary conditions.[19] The shape and dimensions of unit cells containing five functionalized graphene layers with different concentrations of functional groups were systematically obtained by energy minimization.

Additional data for the characterization for the GNR: thermogravimetric analysis (TGA) and Fourier-transform infrared spectroscopy (FTIR), is provided as Supporting Information.

Acknowledgements

The authors are thankful to the Institute of Nanostructures, Nanomodelling and Nanofabrication (Associated Laboratory of the Fundação para a Ciência e a Tecnologia (FCT), Portugal) for funding of the project Grafitran (PEst-C/CTM/LA0025/2011). M. Melle-Franco acknowledges support from FCT through the Ciência 2008 program and grants PEst-OE/EEI/UI0752/2014 and CONC-REEQ. E. Cunha gratefully acknowledges the FCT also for the Ph.D. grant SFRH/BD/87214/2012.

Keywords: graphene · molecular modelling · nanostructures · self-assemble

[1] U. Khan, A. O'Neill, M. Lotya, S. De, J. Coleman, *Small* **2010**, *6*, 864.
[2] D. Li, M. B. Muller, S. Gilje, R. B. Kaner, G. G. Wallace, *Nat. Nanotechnol.* **2008**, *3*, 101.
[3] G. Wang, B. Wang, J. Park, J. Yang, X. Shen, J. Yao, *Carbon* **2009**, *47*, 68.
[4] D. V. Kosynkin, A. L. Higginbotham, A. Sinitskii, J. R. Lomeda, A. Dimiev, B. K. Price, J. M. Tour, *Nature* **2009**, *458*, 872.
[5] A. G. Cano-Márquez, F. J. Rodríguez-Macías, J. Campos-Delgado, C. G. Espinosa-González, F. Tristán-López, D. Ramírez-González, D. A. Cullen, D. J. Smith, M. Terrones, Y. I. Vega-Cantú, *Nano Lett.* **2009**, *9*, 1527.
[6] I. Janowska, O. Ersen, T. Jacob, P. Vennégues, D. Bégin, M-J. Ledoux, C. Pham-Huu, *Appl. Catal. A* **2009**, *371*, 22.
[7] L. Jiao, X. Wang, G. Diankov, H. Wang, H. Dai, *Nat. Nanotechnol.* **2010**, *5*, 321.
[8] L. Ma, J. Wang, F. Ding, *ChemPhysChem* **2013**, *14*, 47.
[9] R. John, D. B. Shinde, L. Liu, F. Ding, Z. Xu, C. Vijayan, V. K. Pillai, T. Pradeep, *ACS Nano* **2014**, *8*, 234.
[10] P. Kumar, L. S. Panchakarla, C. N. R. Rao, *Nanoscale* **2011**, *3*, 2127.
[11] M. C. Paiva, W. Xu, M. F. Proença, R. M. Novais, E. Lægsgaard, F. Besenbacher, *Nano Lett.* **2010**, *10*, 1764.
[12] P. Wagner, V. V. Ivanovskaya, M. Melle-Franco, B. Humbert, J. J. Adjizian, P. R. Briddon, C. P. Ewels, *Phys. Rev. B* **2013**, *88*, 094106.
[13] M. C. Paiva, F. Simon, R. M. Novais, T. Ferreira, M. F. Proença, W. Xu, F. Besenbacher, *ACS Nano* **2010**, *4*, 7379.

[14] J. I. Paredes, S. Villar-Rodil, A. Martinez-Alonso, J. M. D. Tascon, *Langmuir* **2008**, *24*, 10560.
[15] F. Tuinstra, J. Koenig, *J. Chem. Phys.* **1970**, *53*, 1126.
[16] A. C. Ferrari, J. C. Meyer, V. Scardaci, C. Casiraghi, M. Lazzeri, F. Mauri, S. Piscanec, D. Jiang, K. S. Novoselov, S. Roth, A. K. Geim, *Phys. Rev. Lett.* **2006**, *97*, 187401.
[17] K. Strutyński, J. A. N. F. Gomes, M. Melle-Franco, *J. Phys. Chem. A* **2014**, *118*, 9561.
[18] M. J. Dudek, J. W. Ponder, *J. Comput. Chem.* **1995**, *16*, 791.
[19] M. Melle-Franco, M. Prato, F. Zerbetto, *J. Phys. Chem. A* **2002**, *106*, 4795.

Received: December 1, 2014
Published online on March 9, 2015

